Journal of The Electrochemical Society, **149** (10) B472-B478 (2002)
0013-4651/2002/149(10)/B472/7/$7.00 © The Electrochemical Society, Inc.

Synthesis and Corrosion Resistance of High-Silica Zeolite MTW, BEA, and MFI Coatings on Steel and Aluminum

Anupam Mitra, Zhengbao Wang, Tiegang Cao, Huanting Wang, Limin Huang, and Yushan Yan*,z

College of Engineering, Center for Environmental Research and Technology and Department of Chemical and Environmental Engineering, University of California, Riverside, California 92521, USA

High-silica zeolite ZSM-12 $Na_n(Al_nSi_{28-n}O_{56})\sim 4H_2O$ with $n = 2$ (MTW), Beta $Na_n(Al_nSi_{64-n}O_{128})$ with $n = 7$ (BEA), and ZSM-5 $Na_n(Si_{96-n}O_{192})\sim 16H_2O$ with $n < 27$ (MFI) coatings were synthesized by hydrothermal crystallization without seeding using a new two-silica method on Al-alloy (Al-2024-T3 and Al-6061-T4) and stainless steel (SS-304). The pure-silica MTW and BEA coatings synthesized in this study have not been previously reported. All coatings are continuous and have excellent adhesion. The as-synthesized zeolite coatings were tested by a dc polarization technique and found to be highly corrosion resistant in severely corrosive acidic (0.5 M H_2SO_4 aqueous solution) and alkaline (0.1 M NaOH aqueous solution) media. In particular, a pure-silica MFI coating of only a few hundreds of nanometers thickness was formed within a relatively short crystallization time (*e.g.*, 15 min), and was shown to provide sufficient protection against corrosion.
 [DOI: 10.1149/1.1507784]

Manuscript submitted October 9, 2001; revised manuscript received March 21, 2002. Available electronically September 10, 2002.

In recent years there has been considerable interest in the synthesis of zeolite films for membrane and membrane reactor applications.[1-12] Several comprehensive reviews have been published on zeolite membranes.[1-4] Preparation of zeolite films on nonporous substrates for chemical sensor applications[13,14] has been included in these reviews. The inherent molecular sieving capability of zeolites, as amply documented in separation and catalysis applications, has been the primary motivation for these efforts. Recently other interesting applications of zeolite film/coatings have been reported that do not necessarily rely on the molecular sieving effect of zeolites. For example, the significant heat effect associated with adsorption/desorption of water in zeolites (*e.g.*, zeolite X) was considered to be potentially useful for zeolite coating heat pumps.[15] Pure silica zeolite MFI films were demonstrated to be a promising alternative as ultralow-*k* dielectrics for future generation computer chips.[16,17] The mechanical strength of the crystalline zeolites proved superior over other amorphous porous silica low-*k* alternatives such as sol-gel silica and surfactant mesophase templated silica. High-silica MFI coatings with excellent chemical stability have also been shown to be corrosion-resistant and have the potential to replace the heavily polluting chromate conversion coatings that are currently used for the protection of aluminum alloys and steels.[18] In this application, the as-synthesized zeolite coatings containing structure-directing-agent (SDA) are used as a nonporous barrier to corrosive species.

The development of a new environmentally friendly surface finishing technology for corrosion prevention of aluminum alloy and steel is an important area of research.[19-32] Metal corrosion is a serious problem that costs an industrialized country several percent of its gross domestic product (GDP).[33] Sol-gel coatings have been shown to be a promising alternative and are cited for their superior adhesion, good barrier properties, and high thermal and chemical stability.[22-26,28,29] However, sol-gel coatings usually require high-temperature curing that is not compatible with many metal alloys. Also it is difficult to coat surfaces of complex shapes and confined spaces. Electrochemical deposition of conductive polymer coatings is another developing technique for combating corrosion of metal and metal alloys.[30-32] Thermal stability and adhesion are concerns for pure polymer coatings. It has been shown recently that as-synthesized SDA-containing high-silica MFI coatings on aluminum alloys have superior corrosion resistance to chromate conversion coatings in strong acids, bases, as well as pitting aggressive media.[18] It has also been shown that the *in situ* crystallization coating deposition process can coat surfaces of complex shape and confined spaces. In addition, the thermal and mechanical properties of the high-silica MFI coatings were shown to be satisfactory.[34]

In this study, we intend to demonstrate that zeolite coatings could potentially become a general surface finish for combating metal corrosion by showing that in addition to high-silica MFI, other as-synthesized high-silica zeolite coatings can also be corrosion resistant. The two most commonly used metals, steel and aluminum alloy, were tested as the substrates.[35] High-silica zeolites were preferred over low-silica ones because of their high thermal and chemical stability. Three high-silica zeolites with different pore dimensionality, microporosity, and framework density [MTW, BEA, and MFI] were chosen for this study (listed in Table I).[36]

Experimental

Materials.—The substrates used in this study were aluminum alloy 2024-T3, 6061-T4, and stainless steel 304 and are denoted throughout the discussion as Al-2024-T3, Al-6061-T4, and SS-304, respectively. Chemicals used for the synthesis of zeolite coatings included tetraethylorthosilicate (TEOS, 98 wt %, Aldrich), fumed silica (FS, surface area ~ 380 cm^2/gm, 99.8 wt %, Aldrich), silica gel (SG, 35-60 mesh, 99^+ wt %, Aldrich), sodium metasilicate (44-47 wt % silica, Aldrich), colloidal silica (LUDOX, AS-30, Aldrich), tetrapropylammonium hydroxide (TPAOH, 40 wt % aqueous solution, Sachem), tetraethylammonium hydroxide (TEAOH, 35 wt % aqueous solution, Aldrich), triethylmethylammonium hydroxide (MTEAOH, 20 wt % aqueous solution, Aldrich), sodium hydroxide (99.99 wt %, Aldrich), and hydrofluoric acid (HF, 49 wt %, Aldrich).

Substrate pretreatment.—The substrates were mildly polished with 0.3 μm α-Al_2O_3 suspension using a Buehler polisher followed by cleaning with powdered Alconox detergent (Alconox, Inc.). The substrates were then washed thoroughly with deionized water in an ultrasonic bath (5 min) and dried at 373 K.

Coating synthesis.—Cleaned and dried substrates were placed inside the autoclave vertically in such a way that they remained completely immersed in the synthesis gel during crystallization. Square (1.5×1.5 cm) or rectangular substrates (3×2 cm) were used to obtain zeolite coatings. Coatings were synthesized by a direct *in situ* hydrothermal method. Detailed compositions of the synthesis gels are summarized in Table II. No aluminum source was intentionally added to the synthesis gels. Crystallization was carried out at 403 to 448 K for several hours to several days in polytetrafluoroethylene (PTFE) lined (45 mL capacity) Parr 4744 acid digestion bombs.

* Electrochemical Society Active Member.
z E-mail: yushan.yan@ucr.edu

Table I. Zeolite coatings synthesized for corrosion protection under the present study.

Coating type	Template used	Channel system	Framework density	Density[a] (g/cm^3)
MTW	TEAOH	[010] **12** 5.6 × 6.0[b]	19.39 T/1000 Å^3	1.9343
MFI	TPAOH	{[100] **10** 5.1 × 5.5 ↔ [010] **10** 5.3 × 5.6}[c]	17.97 T/1000 Å^3	1.7926
BEA	TEAOH	⟨100⟩ **12** 6.6 × 6.7[d] ↔ [001] **12** 5.6 × 5.6[b]	15.6 T/1000 Å^3	1.5562

[a] Density of zeolite was calculated from framework density data assuming negligible intercrystal void space for siliceous end product; TEAOH, tetraethylammonium hydroxide; TPAOH, tetrapropylammonium hydroxide.
[b] Channel system is one-dimensional.
[c] Channel system is three-dimensional.
[d] Channel system is two-dimensional.

Gel preparation.—Three types of hydrogels were used in this study. For the preparation of the first gel (batch 1-6 in Table II), a clear solution was obtained by the dissolution of sodium metasilicate or sodium hydroxide in deionized water followed by the addition of aqueous TEAOH. After room temperature stirring for 4 h, a silica gel or colloidal silica was added and the final semitransparent liquid mixture was aged for 4 h before being used for coating synthesis.

For the preparation of the second gel (batch 7), fumed silica was first added under stirring to an aqueous solution of TEAOH and the stirring continued until a homogeneous liquid gel was obtained. Then, an aqueous solution of HF was added dropwise to the gel and stirred continuously for several hours to obtain the final gel.

For the preparation of the third gel (batch 8-9), aqueous solutions of TPAOH, NaOH, and deionized water were mixed together and stirred to obtain a homogeneous clear solution. TEOS was then added to the solution followed by room temperature aging for 4 h.

Physical characterization.—The as-synthesized zeolite coatings were flushed with an ample amount of tap water and finally washed under ultrasonication for 10 min. The as-synthesized zeolite coatings were examined with X-ray diffraction (XRD) using a Siemens D-500 diffractometer with Cu Kα radiation. Scanning electron microscopy (SEM) was conducted on a Philips XL-30 electron microscope operated at 20 kV.

DC polarization.—Polarization testing[37] was carried out with a Solartron potentiostat SI 1287 in a three-electrode configuration with the zeolite-coated substrate as the working electrode, a platinum electrode as the counter electrode, and a saturated calomel electrode (SCE) as the reference electrode. The corrosive medium was either 0.5 M H_2SO_4 or 0.1 M NaOH aqueous solution. The edges of the coating were sealed with epoxy while keeping exposed the coating surface whose corrosion-resistance was to be measured. Zeolite-coated samples were immersed in the corrosive medium for 30 min prior to the polarization test.[27] The temperature of the solution during polarization tests was maintained at 298 K. A sweep rate of 5 mV/s[26,37] was applied and all potentials were referred to the saturated calomel electrode (SCE).

Results and Discussion

Synthesis and characterization of high-silica zeolite MTW, BEA, and MFI coatings.—Table II summarizes the typical synthesis conditions for as-synthesized zeolite MTW, BEA, and MFI coatings on Al-2024-T3, Al-6061-T4, and SS-304. High-silica MTW coatings were obtained on Al-2024-T3 and Al-6061-T4 in the presence of TEAOH (batch 1 and 2). When TEAOH was replaced by MTEAOH, similar MTW coatings were obtained. Concentration of OH^- was found to be a crucial parameter in controlling the formation of a pure MTW coating on Al-alloys. An increase in OH^- concentration (with respect to batch 1) causes impurities of MFI and/or BEA in the MTW coating. This is in agreement with the general observation that OH^- plays a critical role in zeolite synthesis.[38] Specifically, at a very high OH^- concentration zeolite BEA layer forms within a 16 h crystallization time, and an increasing crystallization time of 24 h causes growth of a MTW layer over the BEA layer. Corrosion resistance of the BEA coating (in 0.5 M H_2SO_4 solution) obtained after 16 h of crystallization (polarization current quite close to noncoated substrate) was much lower than that of the coating (BEA + MTW) obtained after 24 h of crystallization (polarization current $\geqslant 10^{-7}$). No such effect of OH^- concentration was observed on stainless steel substrates under identical experimental conditions. Further, pure MTW was obtained in the bulk irrespective of the nature of the substrate. Thus, the change in the nature of the coating on an Al alloy substrate at high OH^- concentration is due to the interaction of the substrate and the gel. TEAOH is the most widely used SDA for zeolite BEA synthesis but capable of producing MFI and MTW under suitable conditions.[38] High-silica MTW is much easier to synthesize than high-silica BEA in hydroxyl medium.[38-41] But synthesis of low-silica MTW is difficult.[39,40] OH^-

Table II. Synthesis conditions of zeolite coatings on Al alloys and stainless steel.

Batch no.	Composition	Substrate	$C_{Temp.}$ (K)	C_{Time} (h)	Film type
1	16.4 Na_2SiO_3/100 SiO_2 (SG)/34.4 TEAOH/1795 H_2O	Al-2024-T3	438	24	High silica MTW (thin)
2	23.2 NaOH/100 SiO_2 (SG)/46.4 TEAOH/3934.7 H_2O	Al-6061-T4	438	72	High silica MTW (thin)
3	8.0 Na_2SiO_3/100 SiO_2 (SG)/50 TEAOH/1053.4 H_2O	Al-6061-T4	423	72	High silica BEA (thin)
4	16.7 Na_2SiO_3/100 SiO_2 (SG)/50 TEAOH/2191 H_2O	SS-304	438	16	Pure silica MTW (thin)
5	23.2 NaOH/100 SiO_2 (SG)/46.4 TEAOH/975.2 H_2O	SS-304	438	48	Pure silica MTW (thick)
6	4 Na_2SiO_3/100 SiO_2 (CS)/47.9 TEAOH/1041.5 H_2O	SS-304	413	96	Pure silica BEA (thin)
7	60 TEAOH/100 SiO_2 (FS)/60 HF/977.8 H_2O	SS-304	403	240	Pure silica BEA (thick)
8	2 Na_2O/100 SiO_2 (TEOS)/32 TPAOH/16458.4 H_2O	SS-304	438	4	Pure silica MFI (thin)
9	100 SiO_2 (TEOS)/82 TPAOH/16432 H_2O	SS-304	438	20	Pure silica MFI (thick)

SG-silica gel; FS-fumed silica; CS-colloidal silica; TEOS-tetraethylorthosilicate; thin indicates thickness less than 2 μm whereas thick implies thickness more than 10 μm; $C_{Temp.}$-crystallization temperature; C_{Time}-crystallization time.

concentration of the gel might control the Si/Al ratio on the surface of the substrate at the onset of the film formation on the Al alloy. A higher OH^- concentration might increase participation of Al species in the vicinity of the substrate. Thus, at higher OH^- concentration BEA coating was preferentially formed first. Formation of the initial BEA layer might reduce the influence of the substrate on the film formation and therefore the bulk crystallization process takes over to control the deposition of the MTW layer. In intermediate OH^- concentration, MFI was formed as an impurity. Dilution reduces the rate of crystallization. For example, when batch 1 was diluted 2.9 times (to a composition of 16.4 Na_2SiO_3/100 SiO_2 (SG)/34.4 TEAOH 5000 H_2O), MTW coating was obtained only after 42 h as compared with 24 h without dilution. It is possible that dilution reduced the degree of supersaturation and therefore increased nucleation time.[42] It was observed that coatings on Al alloys have to be formed within a reasonable amount of time to protect the Al alloy from attack by the basic synthesis solution during hydrothermal crystallization. Al alloys suffered heavy corrosion at dilutions higher than 2.9-fold due to the slow crystallization rate. A similar effect of dilution was observed for the composition used in batch 2.

Zeolite BEA coating on Al-6061-T4 was obtained in 3 days at 423 K using a synthesis composition that is closely related to the one for high-silica MTW coatings (batch 3 *vs.* 1). Decreasing sodium metasilicate or increasing TEAOH content of the synthesis composition of batch 1 enhances nucleation of BEA over MTW on Al-6061-T4. Decreasing sodium metasilicate or increasing TEAOH affects OH^- concentration and Na/SiO_2 and/or TEAOH $(SDA)/SiO_2$ ratios, both of which are known to have strong effects on the synthesis of zeolite.[38-43] It has been mentioned earlier that at higher OH^- concentrations zeolite BEA coating was formed preferentially on Al alloy and MTW was deposited as a second layer. It is believed that organic molecules act as pore fillers and Na plays an active role in the nucleation and crystal growth of MTW.[38,40] Unlike BEA,[44] synthesis of zeolite MTW has not succeeded in a hydroxyl medium in the absence of alkali metal ions while using TEAOH as the SDA. Optimum balance between the alkali metal ion and the SDA molecule is necessary for the crystallization of MTW.[40] We believe that increasing the TEAOH concentration enhanced formation of BEA coating while reduction of both sodium and the temperature eliminated bulk crystallization of MTW. At a crystallization temperature of 423 K, the BEA coating has excellent intergrowth (visually and under SEM). Increasing the crystallization temperature from 423 K to 438 K leads to faster formation of BEA coating (data not shown). However, MTW coating quickly forms as a second impurity layer (XRD and SEM data not shown) due to the bulk MTW formation induced by the increasing temperature.

Pure silica MTW coatings (batch 4 and 5) with different thickness were obtained on SS-304 at 438 K. Again the synthesis compositions are closely related to those used for high-silica MTW on Al alloys (batch 1 and 2). The structure-directing agent was TEAOH in both cases. The two synthesis compositions using sodium metasilicate or sodium hydroxide appear fairly versatile in forming high silica MTW coatings on different metals (batch 1 and 2, 4 and 5).

Pure silica BEA coatings (batch 6 and 7) with different thickness were deposited on SS-304 using two distinctively different synthesis compositions. Pure silica BEA has been difficult to synthesize from the commonly used hydroxyl medium. On the other hand, highly hydrophobic pure-silica BEA is easily obtained from the fluoride medium.[45] In this study, pure silica BEA coatings were obtained on stainless steel from both hydroxyl and fluoride media. Synthesis with sodium metasilicate and colloidal silica (batch 6) produced a thin BEA coating within a crystallization time of 96 h. In contrast, a very thick BEA coating with excellent intergrowth was obtained from synthesis in fluoride medium with a crystallization time of 240 h (batch 7).

Pure silica MFI coatings were synthesized on SS-304 within several hours of crystallization (batch 8 and 9). Both thin (batch 8, coating thickness $< 0.5\ \mu m$) and thick (batch 9, coating thickness $> 10\ \mu m$) coatings of pure-silica MFI were obtained on SS-304. While the thin coating of MFI was obtained within 4 h of crystallization, the formation of a thick coating was achieved after a longer crystallization time of 20 h.

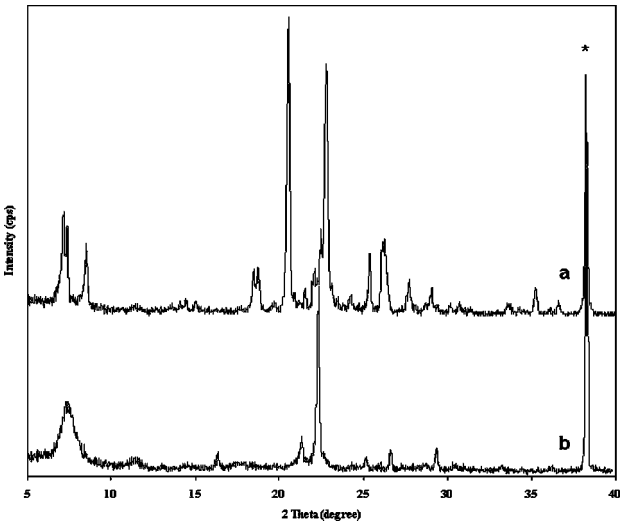

Figure 1. XRD patterns of high silica zeolite coatings on Al-6061-T4: (a) MTW and (b) BEA. Asterisk indicates reflections due to Al-6061-T4.

Zeolite MTW, BEA, and MFI coatings on Al alloys and stainless steel were confirmed by XRD (Fig. 1 and 2). Preferred orientation was observed for the thin MFI coating on stainless steel (Fig. 2e). The *b* axis of the MFI crystals is perpendicular to the stainless steel surface. Figure 3 shows the surface and cross-sectional SEM images of high-silica MTW coatings on Al-6061-T4 (Fig. 3a and b) and high-silica BEA coatings on Al-6061-T4 (Fig. 3c and d). The surface SEM images of different pure silica zeolite coatings on SS-304 are shown in Fig. 4, whereas the corresponding cross-sectional SEM images are presented in Fig. 5. The surface SEM images show that all the coatings are polycrystalline, compact, and continuous. Cross-sectional images provide additional information on the continuity and thickness of the zeolite coatings. The thickness of each coating is marked with a vertical bar in Fig. 3 and 5 for better viewing. The high-silica MTW and BEA coatings on Al alloys are both thin

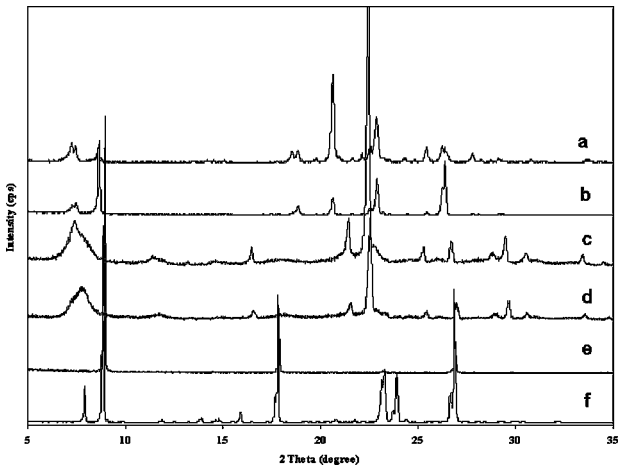

Figure 2. XRD patterns of pure silica zeolite coatings on SS-304: (a) thin MTW coating, (b) thick MTW coating, (c) thin BEA coating synthesized from hydroxyl medium, (d) thick BEA coating synthesized in fluoride medium, (e) thin MFI coating, (f) thick MFI coating.

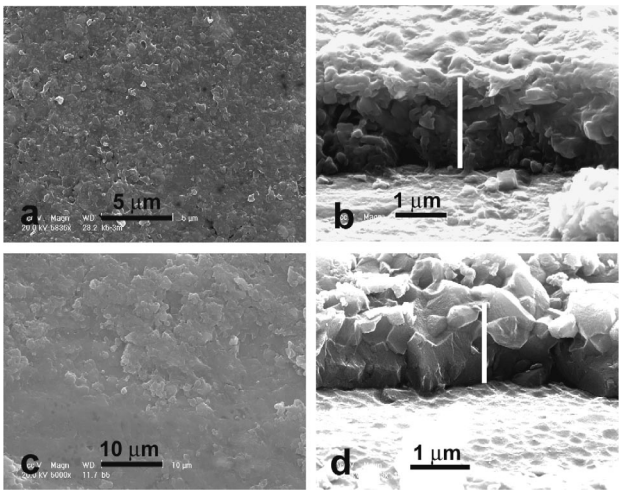

Figure 3. SEM images of different as-synthesized zeolite coatings on Al-6061-T4: (a) MTW coating (surface image), (b) MTW coating (cross section image), (c) BEA coating (surface image), (d) BEA coating (cross section image).

(thickness < 2 μm, Fig. 3) while the thickness of different pure silica coatings on stainless steel varies from about 0.4 μm (Fig. 5e) for MFI to 20 μm for BEA coating (Fig. 5d). The change in crystal size and shape of zeolite coatings with synthesis composition is evident from the SEM images. The thin MFI coating on the stainless steel substrate is composed of plate-like crystals (Fig. 4e and 5e) whereas the MTW crystals are rod-like and elongated (Fig. 4a and 4b, and 5a and 5b). Morphologies of the crystals of other zeolite coatings fall in between these two extremes. It is expected that if

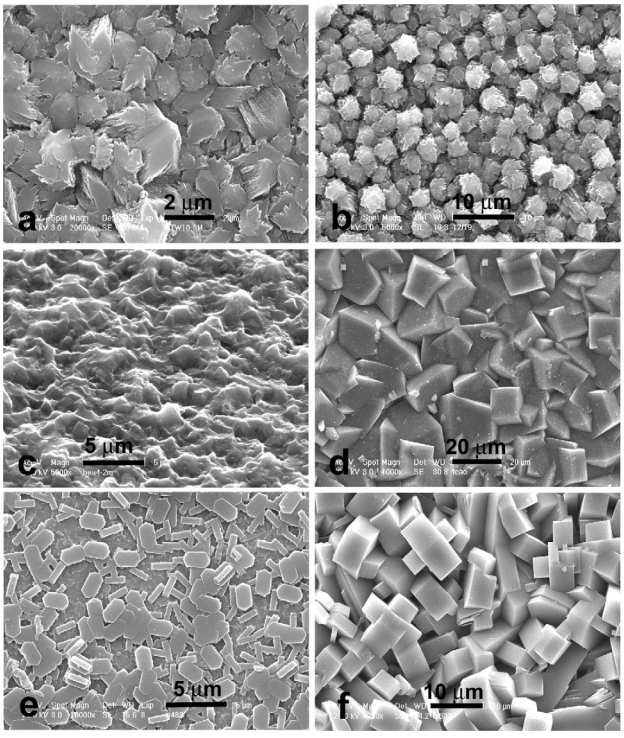

Figure 4. Surface SEM images of different pure silica zeolite coating on SS-304: (a) thin MTW coating, (b) thick MTW coating, (c) thin BEA coating synthesized in hydroxyl medium, (d) thick BEA coating synthesized in fluoride medium, (e) thin MFI coating, (f) thick MFI coating.

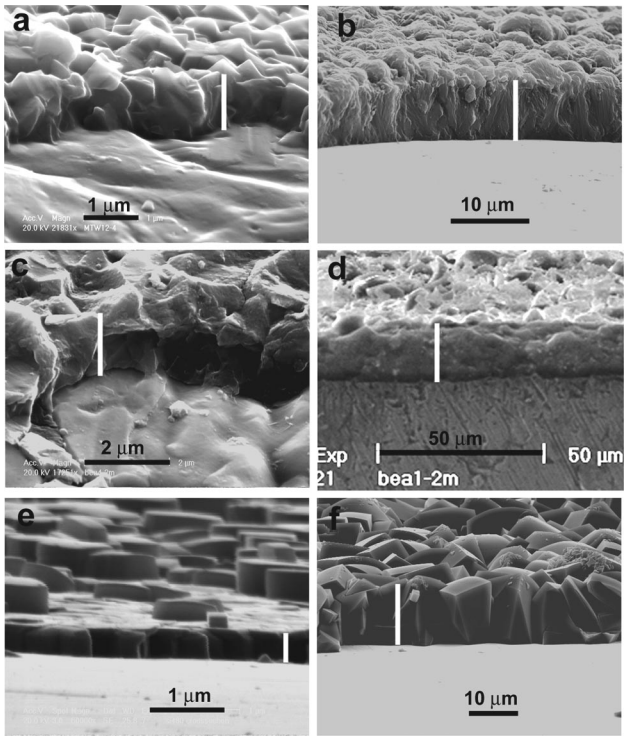

Figure 5. Cross-sectional SEM images of different pure silica zeolite coatings on SS-304: (a) thin MTW coating, (b) thick MTW coating, (c) thin BEA coating synthesized in hydroxyl medium, (d) thick BEA coating synthesized in fluoride medium, (e) thin MFI coating, (f) thick MFI coating.

oriented properly, the plate-like crystals can provide better surface coverage than the rod-shaped or spherical crystals.

Voids and cracks are the most crucial parameter in determining corrosion resistance of a polycrystalline zeolite barrier coating.[35] The formation of voids and cracks are controlled to a great extent by the growth behavior of the coating. It is expected that higher intergrowth leads to higher corrosion resistance. Surface and cross-sectional SEM images confirm the formation of zeolite coatings with excellent intergrowth, although the key parameters affecting intergrowth is not clear at this time. Strong adhesion of the zeolite coating to the metal surface is also of critical importance. Void space at the coating-metal interface is responsible for the accumulation of water and ions at the interface, and believed to be a primary failure mechanism of corrosion resistant coatings.[24] It has been found that the chemical nature of the substrate surface influences nucleation, growth, and adhesion of zeolite crystals.[46] It appears that both Al-alloys and stainless steel can induce a strong gel-substrate interaction during coating formation leading to strongly adhered coatings. Samples for cross-sectional images were prepared either by scratching the surface of the coating with a sharp-edged piece of steel (MTW and BEA coating) or by etching with 49 wt % aqueous HF solution at room temperature for 3-5 s (MFI coating). Strong interaction between the coating and Al alloys and stainless steel was observed from the cross-sectional SEM images of the coatings. In most cases, no clear boundary was observed between the coating and the metal. The coatings appeared to be rooted into the metal surface despite the fact that the samples for cross-sectional SEM images were prepared by a heavy mechanical shock. The strong adhesion also enabled successful polishing of the surface of the zeolite coatings without cracking and delamination (Fig. 6). Polishing experiment reduced surface roughness to a great extent and made the sample suitable for electrical measurements such as dielectric constant measurements. The preparation of all coatings discussed above is highly reproducible although coatings of poor qual-

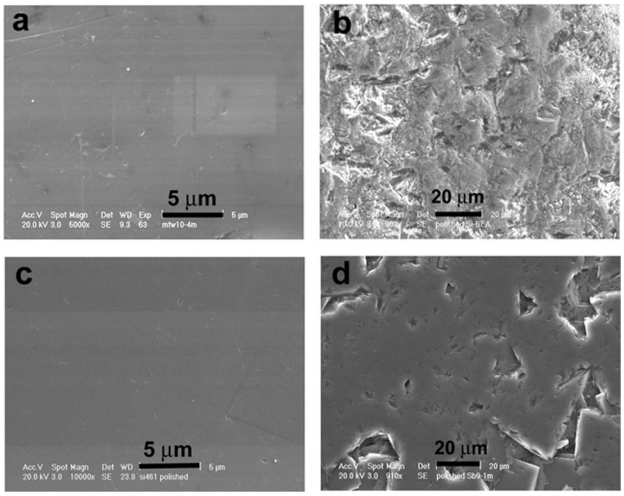

Figure 6. Surface SEM images of different pure silica zeolite coatings on SS-304 after consecutive polishing with sandpaper (3 M 401Q) and 0.3 μm α-Al_2O_3 suspension using a Buehler polisher: (a) thin MTW coating, (b) thick BEA coating synthesized in fluoride medium, (c) thin MFI coating, (d) thick MFI coating.

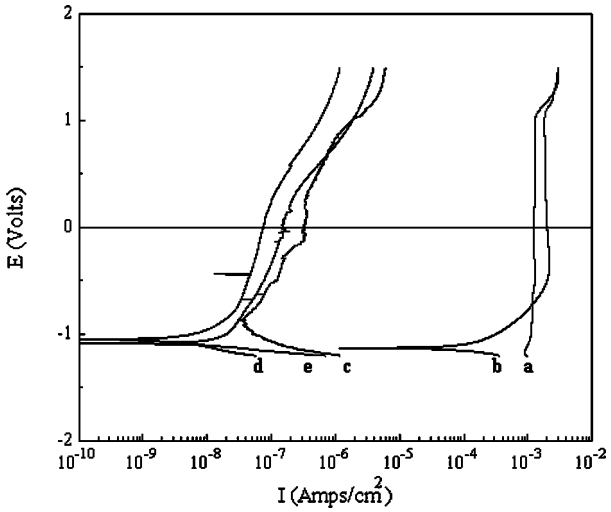

Figure 8. DC polarization curves obtained in 0.1 M aqueous NaOH solution at room temperature from different Al alloys: (a) bare Al-2024-T3, (b) bare Al-6061-T4, (c) high silica MTW-coated Al-2024-T3, (d) high silica MTW-coated Al-6061-T4, (e) BEA coated Al-6061-T4.

ity are produced occasionally due to poor cleaning of the substrate or bad seal of the reactor.

Corrosion resistance of high-silica MTW, BEA, and MFI coatings.—Corrosion resistance of the zeolite coatings was examined by dc polarization, a commonly used technique for corrosion studies.[37] In a typical polarization curve, lower polarization current means high corrosion resistance and vice versa. Corrosion resistance of zeolite MTW and BEA coatings on Al alloys was tested in both acidic (0.5 M H_2SO_4 aqueous solution, Fig. 7) and basic (0.1 M NaOH aqueous solution, Fig. 8) medium. Overall, the polarization currents of the coated samples are three to five orders of magnitude smaller than the noncoated bare Al alloys, indicating good barrier properties of zeolite coatings in both acidic and basic media. MTW and BEA coatings reduced corrosion currents of Al-6061-T4 to a larger extent than MTW coating on Al-2024-T3, suggesting that better coating continuity was achieved on Al-6061-T4. As mentioned earlier, all samples shown in Fig. 7 and 8 were immersed in the corrosive medium for 30 min before the polarization test was carried out. Immersion for longer times (*e.g.*, 2 h) only increases the corrosion current marginally. All the coatings on Al alloys are fairly thin (~2 μm). This clearly shows that a thin zeolite coating is sufficient to significantly reduce corrosion of Al alloys. Coating delamination was not observed after polarization tests under optical microscope or SEM.

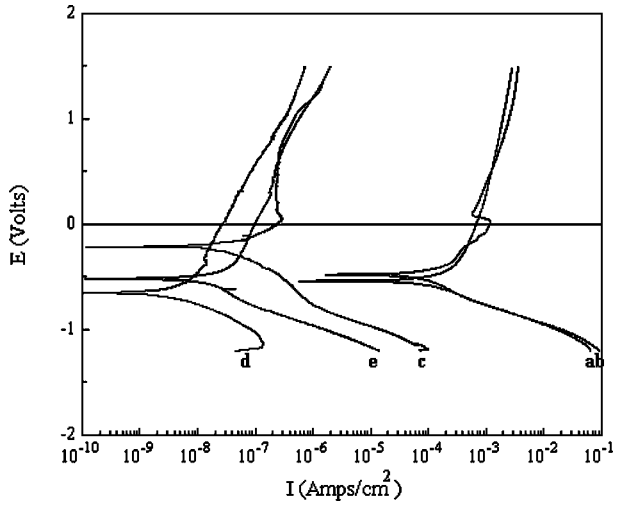

Figure 7. DC polarization curves obtained in 0.5 M aqueous H_2SO_4 solution at room temperature from different Al alloys: (a) bare Al-2024-T3, (b) bare Al-6061-T4, (c) high silica MTW-coated Al-2024-T3, (d) high silica MTW-coated Al-6061-T4, (e) high silica BEA-coated Al-6061-T4.

Figure 9 shows dc polarization curves obtained in 0.5 M H_2SO_4 solution from SS-304 coated with pure silica MTW, BEA, and MFI. As in the case of Al-alloys, reduction in corrosion current of three to five orders of magnitude was observed due to the deposition of zeolite coatings. Among all of the zeolites, the thick coating of pure silica BEA (panel 2) showed the highest corrosion resistance followed by MFI (panel 3) and MTW (panel 1). Similar corrosion currents are expected for all of the zeolite coatings if both the inter- and intracrystal pores are blocked and nonpermeable to the corrosive species. The data obtained in this study seems to suggest the existence of intercrystal porosity within the zeolite coatings. On the other hand, the corrosion currents are quite similar for the thin and thick coatings of MTW (panel 1) and MFI (panel 3) while significantly different for BEA coatings (panel 2). The similar corrosion currents obtained from MTW and MFI coatings with different thickness indicate similar continuity of the zeolite coatings and the polarization tests are free from diffusion limitation. In the case of BEA coatings, the morphology of the coating from the hydroxyl medium is clearly different from the fluoride medium. The growth behavior, continuity, and hydrophobicity of the two coatings are also expected to be different, and this might be responsible for the significant difference in polarization current observed (panel 2).

A conversion coating combined with a polymer topcoat is often used to protect metals and their alloys from corrosion.[35] It is noted that the corrosion resistance of the zeolite coatings synthesized in the present study is comparable or superior to the standard conversion coatings. Coating thickness and deposition time are two important parameters used to evaluate a practical coating. The low polarization current from the thin pure silica MFI-coated SS-304 shows that a zeolite coating of only several hundreds of nanometers in thickness is sufficient to protect the SS-304 surface in a highly corrosive environment. Formation of the thin MFI coating was also relatively fast, *e.g.*, 15 min in a microwave oven or 4 h in a conventional convection oven.

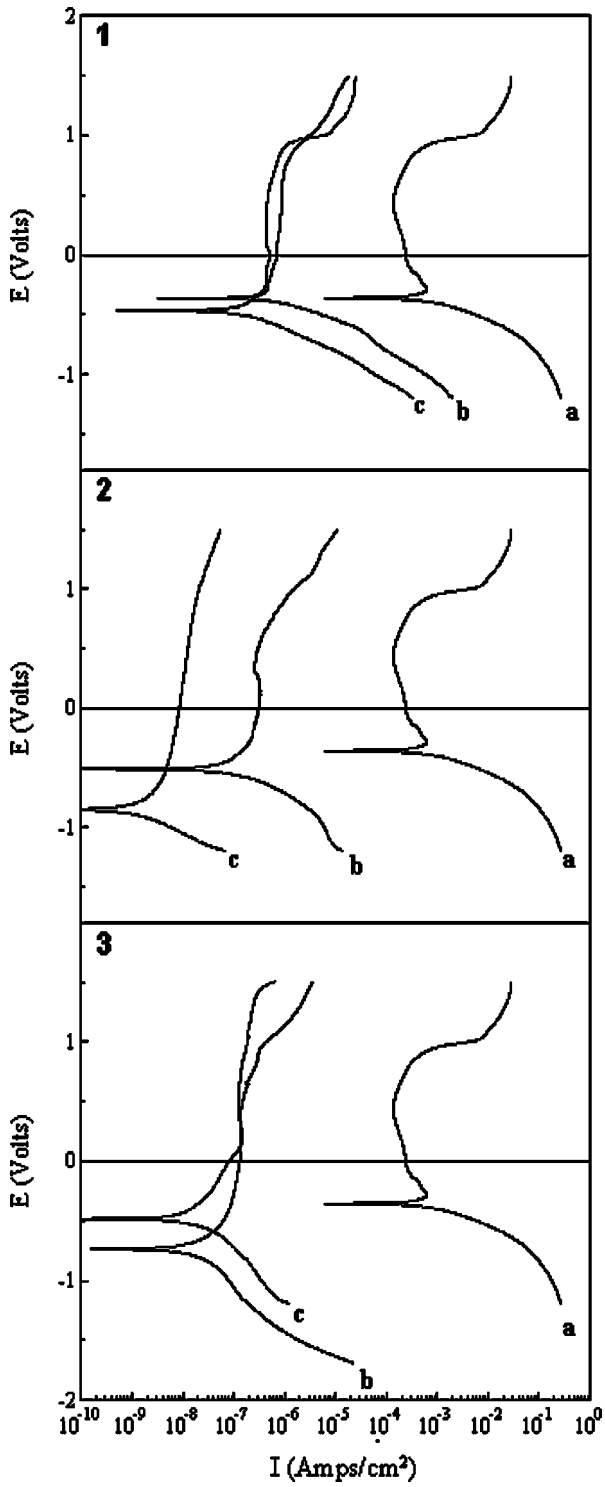

Figure 9. DC polarization curves obtained from (a) bare SS-304, (b) SS-304 coated with thin pure silica zeolite, and (c) SS-304 coated with thick pure silica zeolite in 0.5 M aqueous H_2SO_4 solution. (1) MTW coating, (2) BEA coating, (3) MFI coating.

Conclusions

Highly corrosion resistant continuous high-silica zeolite MTW, BEA, and MFI coatings with excellent adhesion were successfully synthesized using a new two-silica method on Al-2024-T3, Al-6061-T4, and SS-304. The zeolite coatings can protect the metals from corrosion under both acidic and basic environments. Based on the corrosion resistance data of high-silica zeolite BEA, MTW, and MFI coatings, it is reasonable to conclude that high-silica zeolite coatings, in general, can be used as a corrosion resistant coating. The corrosion resistance of zeolite coatings does not seem to depend on the thickness of the coatings, and a coating of a few hundreds of nanometers thickness is sufficient to protect metals and metal alloys from corrosion. The pure-silica MTW and BEA coatings synthesized in this study have not been previously reported and are potentially useful for the preparation of zeolite membranes with interesting separation properties.

Acknowledgments

This research was supported by a grant from the U.S. Environmental Protection Agency's Technology for Sustainable Environment (TSE) program, and by UC-TSR&TP, US-Mexico Materials Corridor Council, UC-SMART, and CE-CERT.

University of California, Riverside, assisted in meeting the publication costs of this article.

References

1. J. Caro, M. Noack, P. Kölsch, and R. Schäfer, *Microporous Mater.*, **38**, 3 (2000) and references therein.
2. A. Tavolaro and E. Drioli, *Adv. Mater.*, **11**, 975 (1999) and references therein.
3. M. Tsapatsis, G. Xomeritakis, H. Hillhouse, S. Nair, V. Nikolakis, G. Bonilla, and Z. Lai, *CaTTech.*, **148**, 3 (2000) and references therein.
4. T. Bein, *Chem. Mater.*, **8**, 1636 (1996) and references therein.
5. T. Sano, Y. Kiyozumi, M. Kawamura, F. Mizukami, H. Takaya, T. Mouri, W. Inaoka, Y. Toida, M. Watanabe, and K. Toyoda, *Zeolites*, **11**, 842 (1991).
6. E. R. Geus, H. Van Bekkum, W. J. W. Bakker, and J. A. Moulijn, *Microporous Mater.*, **1**, 131 (1993).
7. C. S. Bai, M. D. Jia, J. L. Falconer, and R. D. Noble, *J. Membr. Sci.*, **105**, 79 (1995).
8. Y. Yan, M. E. Davis, and G. R. Gavalas, *Ind. Eng. Chem. Res.*, **34**, 1652 (1995).
9. N. Nishiyama, K. Ueyama, and M. Matsukata, *Microporous Mater.*, **7**, 299 (1996).
10. Z. A. E. P. Vroon, K. Keizer, A. J. Burggraaf, and H. Verweij, *J. Membr. Sci.*, **144**, 65 (1998).
11. K. Kusakabe, T. Kuroda, K. Uchino, Y. Hasegawa, and S. Morooka, *AIChE J.*, **45**, 1220 (1999).
12. A. Gouzinis and M. Tsapatsis, *Chem. Mater.*, **10**, 2497 (1998).
13. Y. Yan and T. Bein, *J. Am. Chem. Soc.*, **117**, 9990 (1995).
14. K. J. Balkus, Jr., L. J. Scottile, S. J. Riley, and B. E. Gnade, *Thin Solid Films*, **260**, 4 (1995).
15. M. Tatlier and A. Erdem-Senatalar, *Microporous Mater.*, **34**, 23 (2000).
16. Z. Wang, H. Wang, A. Mitra, L. Huang, and Y. Yan, *Adv. Mater.*, **13**, 746 (2001).
17. Z. Wang and Y. Yan, *Chem. Mater.*, **13**, 1101 (2001).
18. X. Cheng, Z. Wang, and Y. Yan, *Electrochem. Solid-State Lett.*, **4**, B23 (2001).
19. A. Rabbetts, *Trans. Inst. Met. Finish.*, **76**, B4 (1998).
20. J. R. Waldrop and M. W. Kendig, *J. Electrochem. Soc.*, **145**, L11 (1998).
21. J. Zhao, G. Frankel, and G. L. McCreery, *J. Electrochem. Soc.*, **145**, 2258 (1998).
22. M. Guglielmi, *J. Sol-Gel Sci. Technol.*, **8**, 443 (1997).
23. T. L. Metroke, R. L. Parkhill, and E. T. Knobbe, *Prog. Org. Coat.*, **41**, 233 (2001).
24. N. N. Voevodin, N. T. Grebasch, W. S. Soto, F. E. Arnold, and M. S. Donley, *Surf. Coat. Technol.*, **140**, 24 (2001).
25. N. Voevodin, C. Jeffcoate, L. Simon, M. Khobaib, and M. Donley, *Surf. Coat. Technol.*, **140**, 29 (2001).
26. G. P. Thim, M. A. S. Oliveira, E. D. A. Oliveira, and F. C. L. Melo, *J. Non-Cryst. Solids*, **273**, 124 (2000).
27. F. Mansfeld, C. B. Breslin, A. Pardo, and F. J. Pérez, *Surf. Coat. Technol.*, **90**, 224 (1997).
28. M. Mennig, C. Schelle, A. Duran, J. J. Damborenea, M. Guglielmi, and G. Brusatin, *J. Sol-Gel Sci. Technol.*, **13**, 717 (1998).
29. R. Di Maggio, L. Fedrizzi, S. Rossi, and P. Scardi, *Thin Solid Films*, **286**, 127 (1996).
30. J. O. Iroh and W. Su, *Electrochim. Acta*, **46**, 15 (2000).
31. M. Perucki and P. Chandrasekhar, *Synth. Met.*, **119**, 385 (2001).
32. D. Sazou and C. Georgolios, *J. Electroanal. Chem.*, **429**, 81 (1997).
33. R. C. Newman and K. Sieradzki, *Science*, **263**, 1708 (1994).
34. H. Wang, Z. Wang, X. Cheng, A. Mitra, L. Huang, and Y. Yan, *Stud. Surf. Sci. Catal.*, **135**, 22-O-04 (2001).
35. S. Wernick, R. Pinner, and P. G. Sheasby, *The Surface Treatment and Finishing of Aluminum and Its Alloys*, 5th ed., Finishing Publications, Ltd., Teddington, U.K. (1987).
36. Ch. Baerlocher, W. M. Meier, and D. H. Olson, *Atlas of Zeolite Framework Types*, 5th ed., Elsevier, Amsterdam (2001).
37. N. G. Thompson, J. H. Payer, and B. C. Syrett, *DC Electrochemical Test Methods*, Vol. 6, NACE International, Houston, TX (1998).
38. (a) R. Szostak, *Handbook of Molecular Sieves*, Van Nostrand-Reinhold, New York (1992); (b) R. Szostak, *Molecular Sieves*, 2nd ed., Blackie Academic & Professional, London (1998).
39. A. V. Toktarev and K. G. Ione, *Stud. Surf. Sci. Catal.*, **105**, 333 (1997).
40. S. Ernst, P. A. Jacobs, J. A. Martens, and J. Weitkamp, *Zeolites*, **7**, 458 (1987).

41. M. A. Camblor, A. Mifsud, and J. Pérez-Pariente, *Zeolites*, **11**, 792 (1991).
42. D. W. Breck, *Zeolite Molecular Sieves: Structure, Chemistry, and Use*, John Wiley & Sons, New York (1974).
43. R. M. Barrer, *Hydrothermal Chemistry of Zeolites*, Academic Press, New York (1982).
44. M. A. Camblor, A. Corma, A. Mifsud, J. Pérez-Pariente, and S. Valencia, *Stud. Surf. Sci. Catal.*, **105**, 341 (1997).
45. M. A. Camblor, A. Corma, and S. Valencia, *Chem. Commun. (Cambridge)*, **20**, 2365 (1996).
46. J. L. H. Chau, C. Tellez, K. L. Yeung, and K. Ho, *J. Membr. Sci.*, **164**, 257 (2000).